Electromagnetically Controlled Beam-Steerable Reflectarray Antenna

Serup, Daniel E.; Pedersen, Gert Frølund; Zhang, Shuai

Published in:
I E E E Transactions on Antennas and Propagation

DOI (link to publication from Publisher):
10.1109/TAP.2023.3249627

Publication date:
2023

Document Version
Accepted author manuscript, peer reviewed version

Communication

Electromagnetically Controlled Beam-Steerable Reflectarray Antenna

Daniel Edelgaard Serup, Gert Frølund Pedersen, *Senior Member, IEEE*, and Shuai Zhang, *Senior Member, IEEE*

***Abstract*—A beam-steerable 2-bit reflectarray antenna with an electromagnetic control mechanism is presented in this communication. The phase reflection of the proposed 2-bit reflectarray unit elements is altered by moving two pins between a patch and the ground plane. In the suggested concept, the pins are moved with electromagnetism. To prove the concept, a prototype with manually turned screws is evaluated through measurements to verify the reflectarray performance. The prototype antenna is measured to have an impedance bandwidth of more than 5 GHz. The boresight realized gain is measured to be 20 dBi at 25 GHz and a gain bandwidth is more than 2 GHz. Measurements show that the prototype antenna is able to beam-steer in a 120-degree range with a gain drop of less than 3 dB.**

***Index Terms*—Antenna, Reflectarray, Beam-steering, K-Band, mm-wave.**

I. Introduction

Both academic researchers and industry professionals are working on solutions to provide antennas with robust high gain beam-steering at mm-wave frequencies. The literature presents many different methods of achieving beam-steering. They all have different trade-offs between performance, cost, and complexity [1]–[11]. The concept of antenna beam-steering is the art of altering the antenna radiation pattern to aim the peak gain direction of the pattern in different directions. Generally, beam-steering always requires a "change". With different methods, different changes are realized. The change can be a physical movement or rotation. Or, the change can be electrical, such as a variable input signal. With mechanical steering, alignment precision and scanning speed are usually the limiting factors. Since the movement also has to be continuous, large beam direction changes will require a relatively long time to perform. Electrical steering usually has no moving parts and thus has near-instantaneous switching. But, electrical scanning often requires expensive components or very complex biasing structures.

Mechanical beam-steering reflectarray antennas have been investigated in [1]–[5]. The authors in [1], [2] enable reflectarray beam-steering at 12 GHz by moving the reflective surface and the feeding source relative to each other. Aside from the mechanical challenges, the disadvantage of such an antenna configuration is the significant gain drop-off for wider steering angles. **In [1] only a limited $\pm 45^\circ$ steering range is presented and [2] presents a high gain-drop of $\geq$3 dB at 60° steering.** Mechanical reflectarray beam-steering can also be achieved by moving or rotating each unit element individually. In [3], [4] the unit elements of a reflectarray are rotated to generate phase control. In [5] a spring-loaded slider is used to alter the height of the unit elements, which controls the unit element phase response. The disadvantage of these mechanical methods is the size of the control mechanisms. None of these methods would be suitable for mm-wave realizations. Neither the motors nor the spring-loaded mechanisms would be able to be fitted in the available space below a unit element. **The work of [3] uses motors to rotate the unit elements and shows a $\pm$ 40-50° steering range at 8.3 GHz. In [4] manually turned unit elements are used with a 26 GHz design. This antenna shows good steering performance as the $\pm 60^\circ$ steering range only has a 2 dB gain drop. The work of [5] shows a design for 4.82 GHz with very limited beam-steering performance.** Electrically controlled reflectarray beam-steering could be achieved with PIN diode or liquid crystal technology. **In [8]–[10] antennas with PIN-diode controlled beam-steering are presented.** This method is inconvenient since a large number of small electrical components are required. At least one or two PIN-diodes are needed for each unit element. In [11], a liquid crystal controlled reflectarray antenna is studied. Here the phase response of a reflectarray unit element is controlled by applying a bias voltage to a liquid crystal layer in each unit element. Both liquid crystal technology and PIN-diodes will introduce a high loss in the unit elements. And, for mm-wave frequencies, this additional loss will be significant. **The work of [8]–[10] have beam-steering ranges in the interval ± 40 to $\pm 60^\circ$ and are designed for 5, 13, and 10 GHz, respectively. The antenna in [11] operates at 24 GHz, but has a high loss of 4.3dB for a $\pm 45^\circ$ steering range.**

The antenna proposed by this paper is a reflectarray antenna with an electromagnetic control mechanism. An electrical signal is used to generate a magnetic field. The magnetic field will physically move a small metal pin. By moving two actuator pins, the phase response of a 2-bit reflectarray unit element is controllable. Compared to the antennas found in the literature, the proposed antenna will give a new balance between antenna complexity and performance. The antenna will still have moving elements. But with a new novel control mechanism. All moving parts will be encapsulated in the antenna substrate. The antenna will require a large number of control signals and mechanisms. But, unlike **the work of** [8]–[11], the control mechanisms will not introduce a high insertion loss in the unit elements. And, unlike the mechanical solutions proposed in [1], [2], this antenna will provide instantaneous beam-steering.

Manuscript received August 18, 2022; revised October XX, 2022; accepted December XX, 2022. Date of publication September XX, 2023. All authors are with the Antenna, Propagation and Millimeter-Wave Section, Department of Electronic Systems, Aalborg University, 9220 Aalborg, Denmark. (Corresponding author: Shuai Zhang, e-mail: sz@es.aau.dk). This work was supported by the InnovationsFonden Project of MARS2.

II. Electromagnetically Controlled Reflectarray Antenna System

The proposed reflectarray antenna has a feed and a reflective surface. In Fig. 1 a schematic of the antenna is seen. The schematic is a cross-cut of the antenna. The schematic is purely illustrative and it is not to scale. The reflective surface consists of a multi-layer structure with a symmetrical grid of reflectarray unit elements. The proposed reflectarray unit element is a copper patch placed above the ground plane. Each unit element has two movable pin actuators between the patch and the ground plane. The two actuator pins are able to physically move between two positions to change the phase response of the unit element. Each unit element is a 2-bit element since each patch has two pin actuators. A total of four different pin configurations are possible for each unit element. The two pins are able to move up and down from a cavity below the ground plane. In this way, the tip of the screw will either be flush with the ground plane or the pin will be moved up to touch the patch.

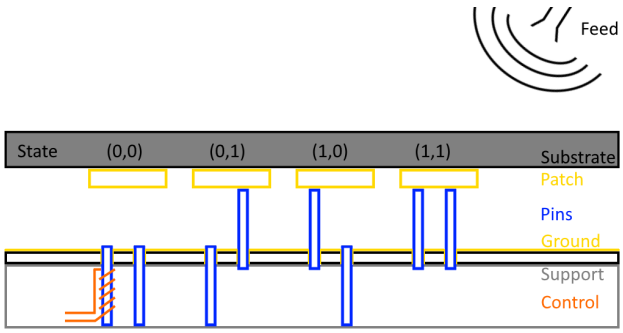

Fig. 1: Schematic showing the four stages of the unit element.

The phase reflection of the unit element will change depending on whether or not the pin actuators are touching the patch. By changing the phase reflection of the unit elements, the phase distribution on the surface layer is also changed. Changing the surface phase distribution, will alter the radiation pattern of the antenna and allow the antenna to achieve beam-steering. In this way, the proposed reflectarray antenna is able to dynamically and instantaneously alter its radiation pattern.

III. Reflectarray Antenna Design

In this section, the proposed reflectarray antenna will be presented. First, this section will present the proposed unit element and summarize its performance. Secondly, it will present the complete configuration of the proposed reflectarray antenna and its beam-steering performance.

A. Unit Element Design

Fig. 2 shows an exploded view of the proposed unit element. The proposed unit element consists of a 3.15 mm square patch centered on the bottom side of a 0.406 mm RO4003 substrate layer. This patch is placed 1 mm above a metal ground-plane block. A middle layer of Polypropylene (PP) material, is used to separate the patch and the ground plane. The last part of the unit element is the two actuator pins. The pins have a diameter of 1 mm. The pin actuators are movable metal cylinders. If moved up, the tip of the two pins will touch the patch +0.8 mm and -1.45 mm from the patch center, along the horizontal center line. The PP separation layer has a 1.2 mm hole above each pin actuator. The holes allow the pin actuators to move through the PP layer.

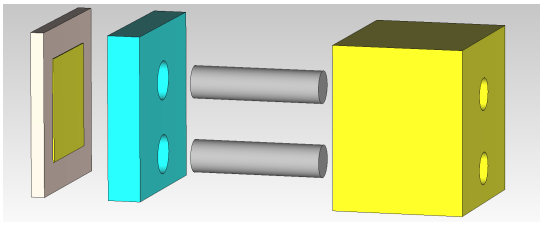

Fig. 2: Exploded view of the proposed unit element. From left to right, the picture shows; the substrate layer with the patch, the PP layer, the pin actuator pins, and the ground layer.

By changing the position of the pin actuators, the phase response of the unit element is altered. Fig. 3 shows four cross-section pictures of the unit element. One picture for each pin setting. Note that a pin in the ”On” position is moved up to touch the patch. And, a pin in the ”Off” position is moved down such that it does not touch the patch.

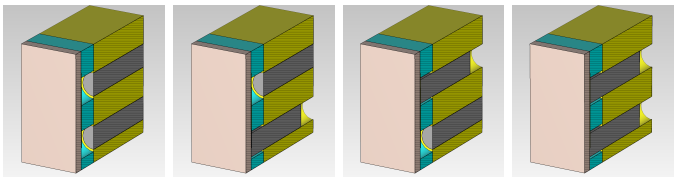

a b c d

Fig. 3: The four stages of the prototype unit element. (a) State 00. (b) State 01. (c) State 10. (d) State 11.

Fig. 4 shows the phase response of the unit element for different frequencies and incident angles. At 25 GHz, the designed unit element covers the full 360° phase rotation with approximately 90° phase difference between the four settings. Overall the unit elements are stable for a wide frequency band and for different incident angles smaller than 30°. However, pin configuration (1,1) does show some frequency sensitivity.

Fig. 5 shows the E-field distribution on the unit element patch for the four different pin settings. As seen from the figures each pin setting result in a different mode. Each mode results in a different phase reflection as the pins ground the patch in different positions.

The physical dimensions of the unit element affect the resulting phase response. The unit element dimensions have been carefully chosen such that the unit element achieves the desired phase response. The best physical dimensions for 25 GHz were found through trial and error by sweeping a large number of different parameter combinations. A simulation of the effect of changing the pin radius and the separation between the patch and the ground plane is seen in Fig. 6. The pin positions together with the patch size only have a relatively small impact and are therefore not shown.

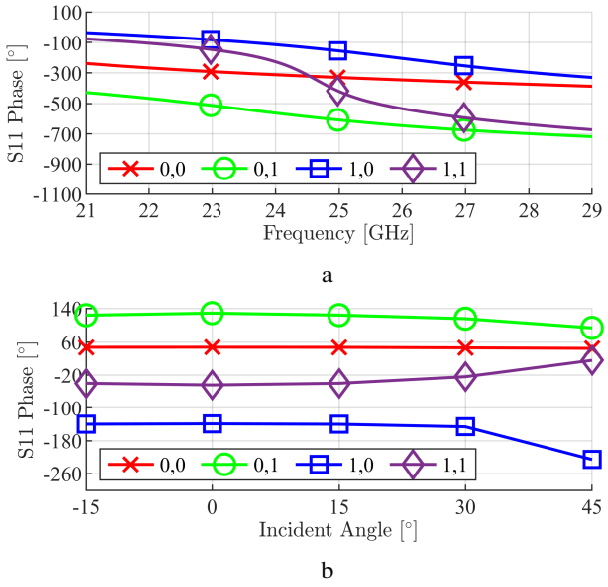

Fig. 4: Simulated phase response of the unit element. (a) Different frequencies. (b) Different incident angles at 25 GHz.

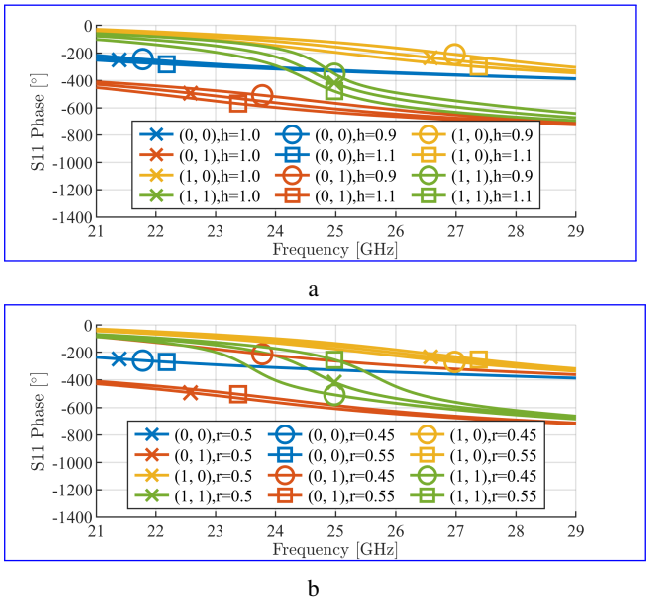

Fig. 6: Parameter sweep of the proposed unit element. (a) Patch separation to ground plane. (b) Pin radius.

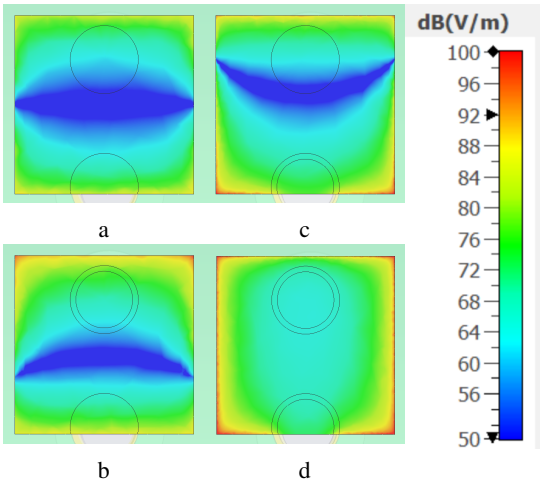

Fig. 5: The E-Field distribution for the unit element. (a) State 00. (b) State 01. (c) State 10. (d) State 11.

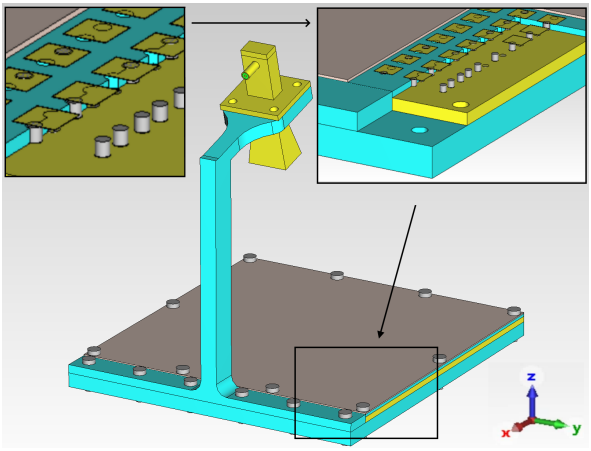

Fig. 7: Simulation model of the proposed reflectarray antenna.

B. Proposed Reflectarray Antenna

Fig 7 shows the simulation model of the proposed reflectarray antenna **designed for 25 GHz** . The proposed reflectarray antenna has a feed and a reflective surface. The feed is a horn antenna that is held by a 3D-printed fixture. The horn is a standard 10 dBi gain horn antenna (Pasternack pe9851/2f-10) [12]. This feed is chosen based on its availability to the author. The feed horn is placed 70 mm above the surface with a 20 mm offset in the x-axis (Forwards the fixture mount). The reflective surface area of the antenna is 100 by 100 mm. The surface is a multi-layered structure that houses 400, 2-bit reflectarray unit elements arranged in a symmetrical 20 by 20 grid. The three antenna layers are kept tightly together by the M2.5 screws seen along the edge of the antenna surface.

C. Antenna Beam-Steering Performance

The proposed antenna can realize any steering direction by changing the configuration of the actuator pins. It would be impossible to test all possible steering directions, therefore, only a few different directions are investigated. Fig. 8 shows the phase distributions and the resulting simulated radiation patterns for three steering directions. Wide beam-steering with high gain can be observed clearly as the realized gains of the three radiation patterns are 22.8, 20.2, and 19.7 dBi, respectively.

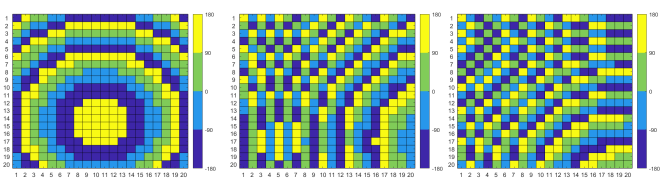

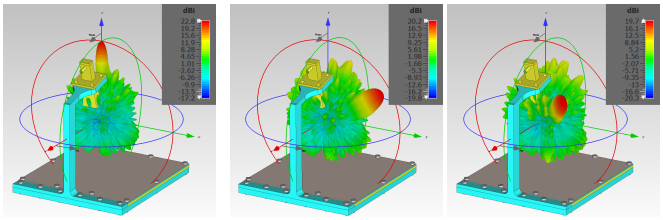

d e f

Fig. 8: The phase distributions and the resulting simulated radiation patterns for three steering directions. (a & d) Boresight. (b & e) $(\theta, \phi) = (60°, 80°)$. (c & f) $(\theta, \phi) = (60°, 45°)$.

Fig. 9 and Fig. 10 show the beam-steering performance of the proposed antenna. The steering performance is good, but some blockage from the feed and its mounting fixture is observed. From the shown simulation results, it is seen that the proposed antenna is able to beam-steer to even large angles and that the gain remains acceptable for a large frequency range. The sidelobe level of the antenna depends on the beam-steering angle. For most directions, the proposed antenna has a sidelobes level of more than 14 dBi, but a few directions only achieve an 8 dBi sidelobe level. The radiation efficiency is above 90% for all steering directions in the frequency range from 24 to 29 GHz.

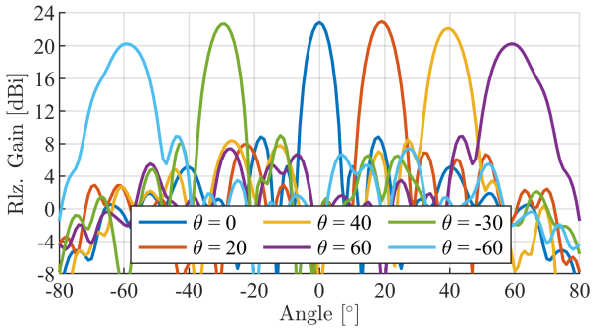

a

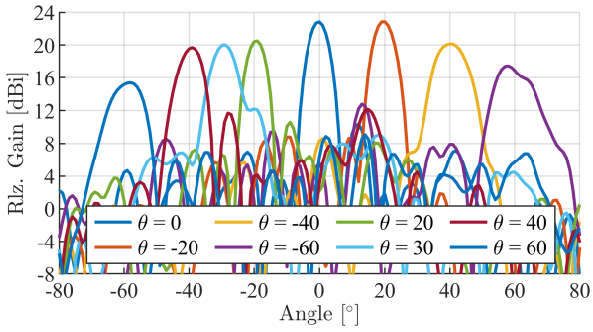

b

Fig. 9: Simulated beam-steering performance.
(a) The yz-plane ($\phi = 90°$). (b) The xz-plane ($\phi = 0°$).

IV. Unit Element Control Investigation

The pin actuators should be moved with electromagnetism by using substrate-integrated coils. The idea behind the proposed unit element control mechanism is inspired by the working principle of a solenoid. A very simplified solenoid has two components. A coil of conductive material and a metallic cylindrical core. The core is located inside the coil structure. If a direct electrical current is passed through the coil, a magnetic field will form around the coil. The center of the core will be magnetically attracted to the center of the magnetic field created by the coil. Thus, the core will seek to move to the center of the coil. [13], [14]

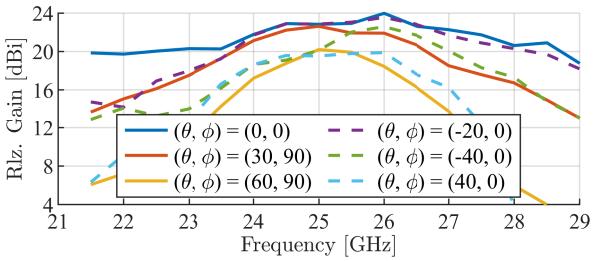

Fig. 10: Realized gain for different steering directions.

Fig. 11 shows different views of the proposed substrate-integrated coil design. Two substrate-integrated coils are needed for each pin. One coil will move the pin to the ”on” position and another coil will move the pin to the ”off” position. As seen from Fig. 11 the coil structures are located below the ground plane, and they are therefore completely isolated from the unit element patches on the other side of the ground plane. The coil coupling and the static fields generated by the coils will be completely isolated and will not have any effect on the phase reflection of the unit elements. The static fields from the coils could be completely encapsulated in a grounded shield if the use case applications benefit from this. The unit element is modeled as having a flat contact point between the pin and the patch. If the contact point is moved or altered, it will slightly impact the phase curves. However, this effect can easily be counteracted by tuning the other unit element dimensions such as the pin radius.

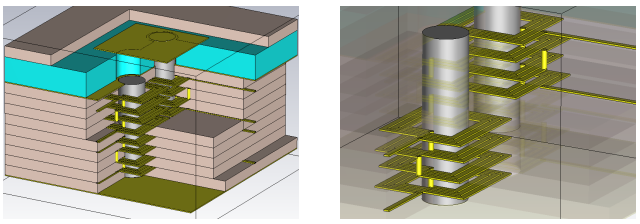

a b

Fig. 11: The substrate integrated coil structure. (a) Model with parts of the structure removed to highlight the internal structure. (b) Model with two of the four coil structures highlighted.

The unit element seen in Fig. 11 is simulated using the Magnetostatic Solver (Ms-Solver) in CST Studio Suite 2021. This solver is a 3D solver designed to simulate static magnetic fields. By applying a direct current to the two terminals of the substrate-integrated coil, it is possible to simulate how much force the magnetic field created by the structure will affect the pin actuator. The simulation shows that the designed coils

should be capable of moving the pin actuator between the on and off positions. Fig. 12 shows the simulated pulling strength of the proposed substrate integrated coil.

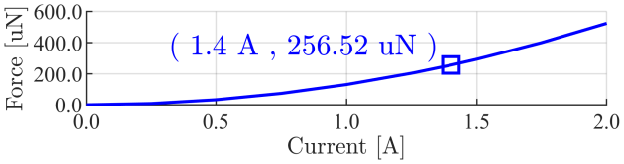

Fig. 12: Simulated pulling strength of the proposed substrate integrated coil.

V. Experiment and Discussion

In this section, the fabricated antenna prototype will be presented and evaluated. The measured and simulated performance of the fabricated antenna prototype will be compared.

A. Antenna Prototype

Due to limited time and resources, a simplified unit element has been used for the antenna prototype. The simplified unit element used 1M screws as the pin actuators. The ground plane is made of brass and has two small 1 mm threaded holes for each unit element. Fig 13 shows pictures of the fabricated antenna prototype.

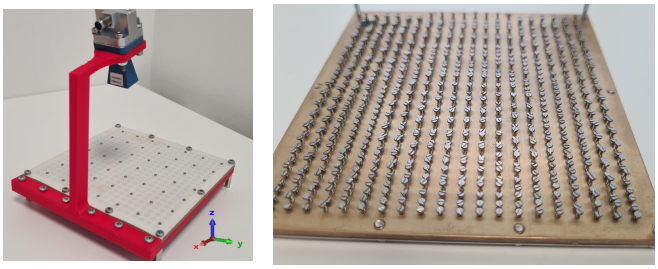

a b

Fig. 13: The antenna prototype. (a) Top view. (b) Bottom view.

For the pin actuators to operate correctly it is vitally important that the pin makes physical contact with the patch. Doing prototype measurements it was found that it was very challenging to guarantee good physical contact for all screws simultaneously. It is very easy to over-tighten the screw and bend or even penetrate the substrate. If a screw is over-tightened and the substrate lifts in one place, it might result in the screw not touching correctly in the neighboring positions. This meant that the prototype had to be modified after fabrication to achieve reasonable results. Therefore, a series of small M1 screws were added to the top of the substrate to prevent it from bending and lifting. Thus the difference between the proposed antenna and the prototype is the addition of the top screws. It should be noted that, if the proposed electromagnetic solution is implemented, this problem would probably be solved. The magnetic forces of the substrate-integrated coils are much lower and more precisely controlled than the forces applied by manually turning a screwdriver.

B. Measured Antenna Performance

This section will give a comparison between the measured and simulated performance of the prototype antenna. The difference between the proposed antenna and the prototype antenna is the addition of the top screws, as described in the previous subsection. To add the additional screws some of the unit elements had to be removed and some performance was sacrificed.

Fig. 14 shows the impedance match when steering in a few different directions. It is seen that the impedance match is wider than 5 GHz for all measured steering angles.

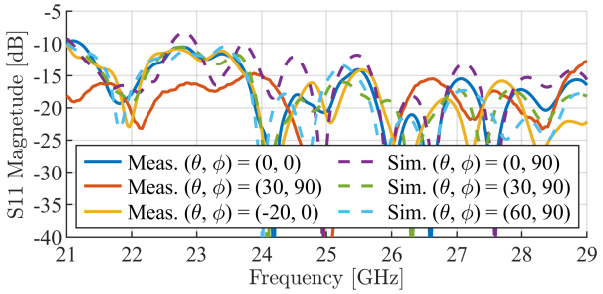

Fig. 14: S11 of the antenna prototype for different directions.

Fig. 15 and Fig. 16 show the simulated and measured beam-steering performance of the antenna prototype. The measured gain of the prototype is within 1 dB from the simulation of the prototype in all cases. **The measured maximum realized gain is 20 dBi and the measured 60° steering angle shows a 2.9 dB gain drop.**

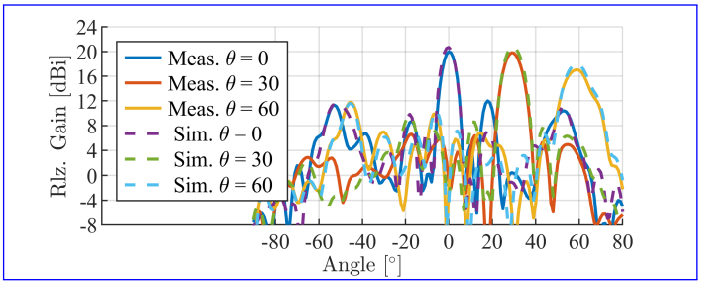

Fig. 15: Beam-steering in the yz-plane ($\phi = 90°$).

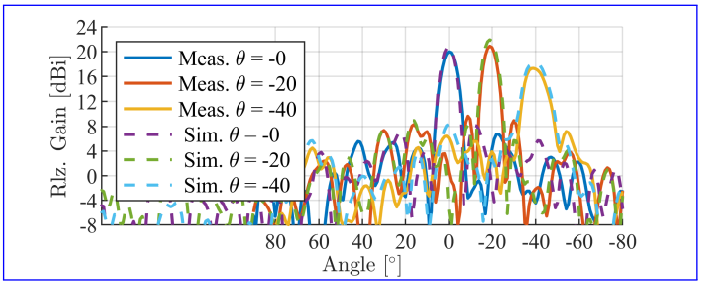

Fig. 16: Beam-steering in the xz-plane ($\phi = 0°$).

The frequency-dependent gain at a few different steering directions is shown in Fig. 17 and Fig. 18. The measured performance is similar to the expected from the simulation. However, it is about 1.5 dB lower at some frequencies.

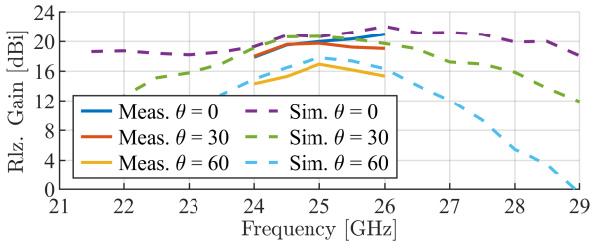

Fig. 17: Realized gain for $\phi = 90$ steering directions.

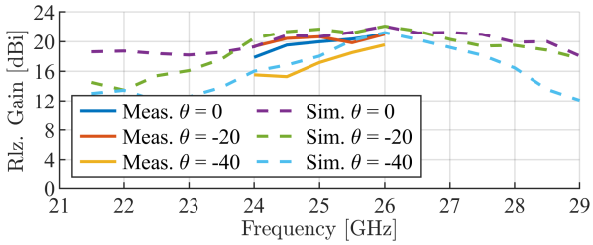

Fig. 18: Realized gain for $\phi = 0$ steering directions.

C. Measurement Conclusion

The measured antenna performance is in good agreement with the simulation model of the antenna prototype. The measurement proves that the designed unit element functions and performs as expected from the simulation.

The addition of the top screws does have an impact on the performance of the antenna. For further development of the antenna, special attention should be put into ensuring that the substrate does not bend. This will remove the requirement to install the top screws. Since the force provided by the substrate-integrated coil is low and controllable, it is not expected that the problem will remain when the proposed electromagnetic control mechanism is implemented. For future development, a multilayer glues substrate configuration would further reduce the flexibility of the top substrate layer.

VI. Comparison with State-of-the-art

Tab. I shows a performance comparison between the antennas proposed by this paper compared with various antennas found in the state-of-the-art literature. It is seen how the proposed antenna achieved good resulting performance compared with the other antennas. The antenna achieves a wider steering range or a lower scanning range loss than any of the other analyzed antennas found in the state-of-the-art.

VII. Conclusion

This paper has presented a unique reflectarray antenna design. A novel unit element control mechanism to enable electromagnetically controlled beam-steering has been presented. The proposed reflectarray antenna uses 2-bit unit elements. The phase reflection of the unit elements is altered by physically moving two pin actuators for each unit element. The proposed solution is to move the pin actuators with the electromagnetic forces generated from a substrate-integrated coil.

TABLE I: Performance comparison between the proposed antenna and other antennas found in the state-of-the-art literature.

Antenna	*CF[GHz]*	*RG[dBi]*	*AE*	*GD[dB]*	*SR[°]*
Proposed	25	22.8	21.8	2.6	±65°
Sim. Prot.	25	20.7	13.5	2.8	±62°
Meas. Prot.	25	20.0	11.5	2.9	±60°
[1]	12	25.4	43.1	-	±45°
[3]	8.3	29.2	35.0	4.3	-
[9]	13	21.4	15.8	3.6	-
[10]	10	24.4	21.9	-	±45°
[11]	24	20.2	23.1	-	±45°
Note: Center Frequency (CF), Realized Gain (RG), Aperture Efficiency (AE), 60° Steering gain drop (GD), -3 db Steering range (SR)					

A proof-of-concept prototype antenna has been manufactured and measured. A good agreement between simulation and measurement has been observed. A good realized gain and a low steering loss have been measured even for very large steering angles. The prototype antenna is measured to have an impedance bandwidth of more than 5 GHz. Measurements show that the prototype antenna is able to beam-steer in a 120-degree range with a gain drop of less than 3 dB.

References

[1] G. Wu, S. Qu and S. Yang, "Wide-angle beam-scanning reflectarray with mechanical steering," *IEEE Trans. Antennas Propag.,* vol. 66, no. 1, pp. 172-181, Jan. 2018.

[2] G. -B. Wu, S. -W. Qu, S. Yang and C. H. Chan, "Low-cost 1-D beam-steering reflectarray with ±70° scan coverage," *IEEE Trans. Antennas Propag.,* vol. 68, no. 6, pp. 5009-5014, June 2020.

[3] X. Yang et al., "A broadband high-Efficiency reconfigurable reflectarray antenna using mechanically rotational elements," *IEEE Trans. Antennas Propag.,* vol. 65, no. 8, pp. 3959-3966, Aug. 2017.

[4] P. Mei, S. Zhang and G. F. Pedersen, "A low-cost, high-efficiency and full-metal reflectarray antenna with mechanically 2-D beam-steerable capabilities for 5G applications," *IEEE Trans. Antennas Propag.,* vol. 68, no. 10, pp. 6997-7006, Oct. 2020.

[5] X. Yang et al., "A mechanically reconfigurable reflectarray with slotted patches of tunable height," *IEEE Antennas Wireless Propag. Lett.,* vol. 17, no. 4, pp. 555-558, April 2018.

[6] Z. -Y. Yu, Y. -H. Zhang, S. -Y. He, H. -T. Gao, H. -T. Chen and G. -Q. Zhu, "A wide-angle coverage and low scan loss beam steering circularly polarized folded reflectarray antenna for millimeter-wave applications," IEEE Trans. Antennas Propag., vol. 70, no. 4, pp. 2656-2667, April 2022.

[7] M. Ettorre, R. Sauleau and L. Le Coq, "Multi-meam multi-layer leaky-wave SIW pillbox antenna for millimeter-wave applications," *IEEE Trans. Antennas Propag.,* vol. 59, no. 4, pp. 1093-1100, April 2011.

[8] J. Han, L. Li, G. Liu, Z. Wu and Y. Shi, "A wideband 1 bit 12 x 12 reconfigurable beam-scanning reflectarray: Design, fabrication, and measurement," *IEEE Antennas Wireless Propag. Lett.,* vol. 18, no. 6, pp. 1268-1272, June 2019.

[9] Y. Wang, S. Xu, F. Yang and M. Li, "A novel 1 Bit wide-angle beam scanning reconfigurable transmitarray antenna using an equivalent magnetic dipole element," *IEEE Trans. Antennas Propag.,* vol. 68, no. 7, pp. 5691-5695, July 2020.

[10] H. Luyen, Z. Zhang, J. H. Booske and N. Behdad, "Wideband, beam-steerable reflectarrays based on minimum-switch topology, polarization-rotating unit cells," *IEEE Access,* vol. 7, pp. 36568-36578, 2019.

[11] X. Li et al., "Broadband electronically scanned reflectarray antenna with liquid crystals," *IEEE Antennas Wireless Propag. Lett.,* vol. 20, no. 3, pp. 396-400, March 2021.

[12] WR-34 waveguide standard gain horn antenna (PE9851/2F-10) by Pasternack Enterprises Inc.

[13] Mark Mancini, "How solenoids work", Jan 13, 2021.

[14] The Engineering Mindset, "Solenoid basics explained - Working Principle", YouTube. 25. mar. 2019.

[15] D. E. Serup, G. F. Pedersen and S. Zhang, "Dual-band shared aperture reflectarray and patch antenna array for S- and Ka-bands," *IEEE Trans. Antennas Propag.,* vol. 70, no. 3, pp. 2340-2345, March 2022.